



Fault induced rock bursts and micro-tremors – Experiences from the Gotthard Base Tunnel



Michael Rehbock-Sander*, Thomas Jesel

Amberg Engineering AG, Trockenloostraße 21, 8105 Regensdorf-Watt, Switzerland

ABSTRACT

During the construction of the Faido Multifunction Station of the Gotthard Base Tunnel, a previously unknown and unanticipated major tectonical fault has been encountered. Upon completion of the advance through the fault, systematic and major rock burst events occurred in the competent Gneiss rock mass adjacent to the fault.

The Swiss Earthquake Service (Schweizer Erdbebendienst – SED) observed an increase of microtremors in the vicinity of the tunnelling site, in a region where usually very low seismic activity is present. As a consequence, the seismic monitoring grid has been enhanced in the project area, allowing reliable pin-pointing of the microtremor hypocenters and examination on the interaction with the tunnel advance and the observed rock burst events.

Due to the vast amount of scientific work with regard to rock burst causes, classification, prediction and mitigation, this publication deliberately abstains from trying to add yet another set of relationships and/or classification schemes. Instead, a case study is presented, with the peculiarity that excellent seismic monitoring and very well documented rock mass conditions are seamlessly available, allowing direct correlation and insight into the interaction between seismicity and strike-slip rock bursts. In addition, the results of a dynamic analysis performed in UDEC, with excitation wave data and rock mass parameters calibrated on the field measurements, are presented. They allow greater understanding of the events caused by seismicity-induced rock burst phenomena.

The experiences with prediction and mitigation of rock burst are shown, leading to conclusions with regard to efficient and safe tunnelling in rock-burst prone rock masses.

1. Introduction

The Gotthard Base Tunnel (GBT) is the core of the NEAT (New Railway Link through the Alps, NRLA). The entire 57 km long tunnel is divided into five construction sections in order to attain a reasonable construction time and for ventilation purposes. Excavation started from the portals at Erstfeld and Bodio as well as from three intermediate attacks located in Amsteg, Sedrun and Faido (Fig. 1).

The tunnel consists of two parallel single-track tubes which are linked by cross-passages every 300 m. Two multifunction stations are located at one-third and two-thirds of the tunnel length. These will be used for the diversion of trains to the other tube via crossover tunnels, to house technical infrastructure and equipment and as an emergency station for the evacuation of passengers. More information can be found at www.alptransit.ch.

During the construction of the Faido MFS, frequent and often massive rock bursts have occurred since March 2004. In addition, the Swiss Seismological Service (SED) recorded an accumulation of seismic activity in the area of the Faido MFS. In July 2005, the owner of the tunnel, ATG (AlpTransit Gotthard AG), formed a working group called ‘Micro-Tremors’ to investigate all aspects related to the seismic activity, especially the impact of a seismic event on the tunnel under operation,

the first author was heading this working group.

The event history of the observed rock burst events during the construction, the analysis of the mechanisms involved, the findings of the working group, the implemented mitigation measures and the assessment of long-term behaviour will be discussed in the course of the paper.

2. General information and initial difficulties

2.1. Geological and geotechnical conditions

From north to south, the GBT passes through mostly crystalline rock, the massifs which are interrupted by narrow sedimentary tectonic zones. The three crystalline rock sections include the Aare massif to the north, the Gotthard massif and the Penninic gneiss zone to the south. These massifs consist mainly of high-strength igneous and metamorphic rock. More than 90% of the total tunnel length consists of these types of rock. The maximum overburden is about 2350 m (Fig. 1).

The location of the Faido MFS was originally predicted in Leventina gneiss of good quality. The outcrops from quarries in the area of the Faido MFS, the experience made during construction of the investigation system for the Triassic Piora basin as well as vertical exploration

* Corresponding author.

E-mail addresses: mrehbock@amberg.ch (M. Rehbock-Sander), tjesel@amberg.ch (T. Jesel).

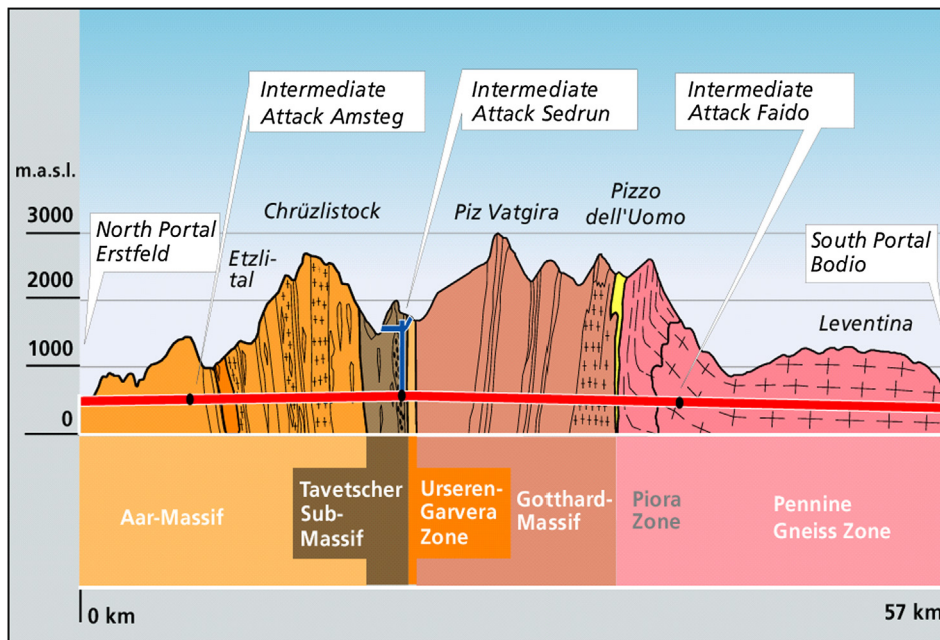


Fig. 1. Geological longitudinal profile of the GBT.

drilling confirmed a favourable geological section.

The identified most relevant hazards for the Faido MFS were:

- Block detachment (brittle failure): The danger of detaching wedges depends on the frequency, distance and quality of joints and discontinuities in the rock mass.
- Loosening: in highly jointed rock mass loosening can occur in the crown area. The loosened rock mass is additionally loading the support and the lining and/or influences the bedding of the support adversely.
- Squeezing: (plastic deformations): Squeezing properties in deep tunnels in hard rock normally are to be expected in the mylonitic and cataclastic zones of fault zones.
- Rockburst: (brittle failure)

2.2. Initial difficulties during construction

During the construction of the cross-cavern, a breakdown of fine-grained quartz occurred in the cavern roof forming a cavity of 8 m in height. Simultaneously severe deformation problems occurred totally unexpected in the heading of the northern logistic gallery. The heading works had to be stopped due to stability problems. This heading took place in the section where the crossover caverns should be positioned in the main tunnels with cross sections up to 250 m². Therefore, extensive exploration drillings and seismic reflection measurements were conducted during further construction. The results of these investigations revealed an until then unknown large fault system in the area of the Faido MFS. The main kernel of this fault strikes at an average angle of about 20° to 15° to the tunnel axis and dips at about 80° to the east (Fig. 2). In the fault's kernel, layers of partially completely decomposed rock (kakirite) are embedded. Adjacent to the east of the fault, hard and brittle Leventina gneiss is located. To the west of the fault, the rock mass consists of hard but less brittle Lucomagno gneiss.

As a result of the aforementioned investigations, it was decided to adapt the layout of the Faido MFS with the aim of placing the large caverns in good rock conditions. Different alternative layouts were investigated. Finally, the branch-off structures were shifted to the southern part of the MFS (Fig. 2).

Besides the layout of the MFS, the geology encountered also made it necessary to carry out a critical review of excavation support means to

be applied in the relevant cross-sections. With the initially designed support consisting of pattern bolting steel meshes and shotcrete, no stability could be achieved in the single-track tunnel west/north (EWN). Therefore, the section of the EWN tunnel was rebuilt with a support consisting of HEM 200 steel arches backfilled with 40 cm of concrete. The support was installed immediately after each excavation step of 1 m. This rigid support was intended to cater for the heavy pressure and especially to protect the workforce from break in the working area. However, the displacements developed immediately after excavation. In the rebuilt section, on a length of 250 m from the cross-cavern to the north, the loading of the support gave rise to displacements of up to 1 m. Strain measurements revealed yielding of the steel arches already four days after backfilling. Severe damage of the support developed (Fig. 3) and the critical section had to be rebuilt again with an enlarged excavation radius of 1.5 m to allow for additional displacements. A flexible support had been successfully installed. TH profiles with sliding connections were used. Horizontal shotcrete slots at the level of the arches' clutches were left open for unhindered sliding of the arches and to avoid damage of the shotcrete lining in case of increasing displacements (Fig. 4).

In order to better understand the failure mechanisms in the area around the tunnels of the MFS, numerical modelling was carried out (static load case). The model section is indicated in Fig. 2. The investigation was based on a parametric study comprising the variation of rock and joint properties. The 2D UDEC model is shown in Fig. 5. The different fault regions in the model have been selected according to the geologist's findings based on interpretation of borehole results. The material parameters are specified in Table 1 (IGGBTS, 2008). For the EWN tube an excavation support with discretized elements (70 cm concrete) was implemented in the model. Additionally an inner concrete lining with liner elements was modelled for both tubes (EON 35 cm, EWN 60 cm).

The results clearly show a considerable extension of the stress redistribution due to the excavation of the tunnels and stress concentration generated in the competent rock mass adjacent to the fault.

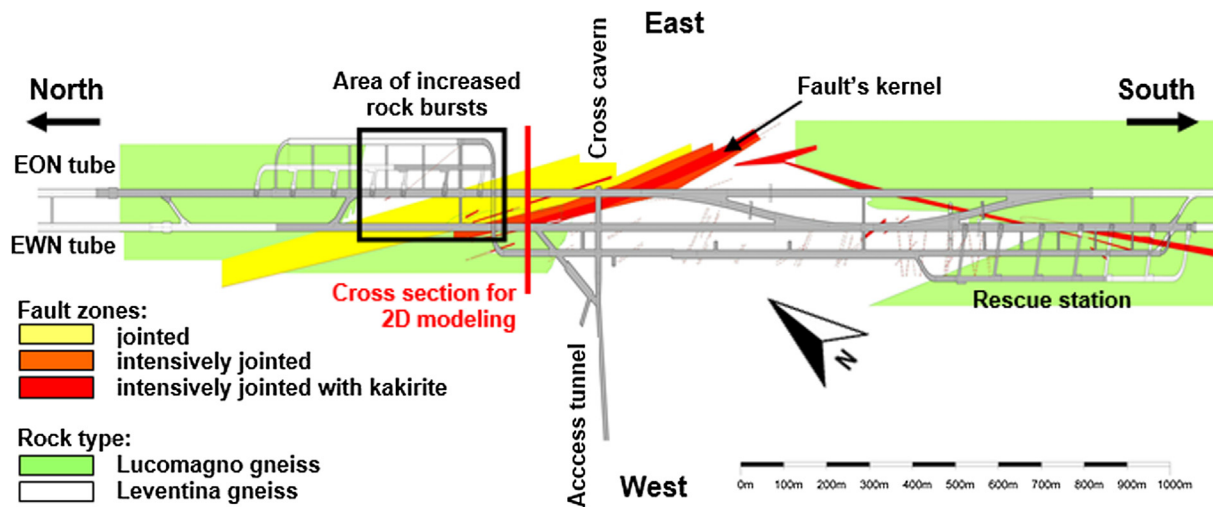


Fig. 2. Faido MFS, with the geological conditions recognised during construction.

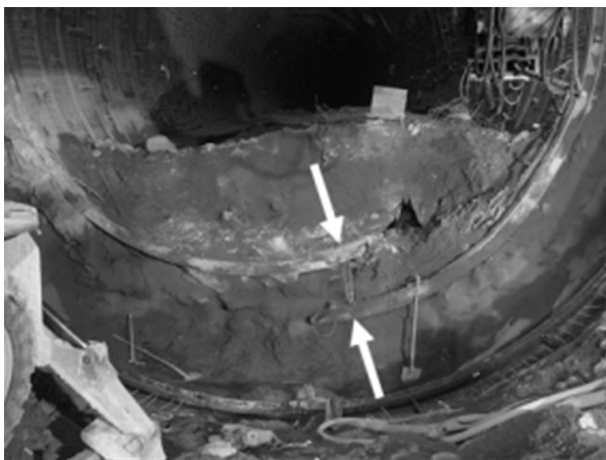


Fig. 3. Sheared-off steel arch in the invert.



Fig. 4. Reprofilling the critical section.

3. Micro – Seismicity and rock bursts

3.1. Development of the seismic activity

Between March 2004 and June 2005, the Swiss Seismological Service (SED) recorded an accumulation of seismic activity in the area of the Faido MFS, normally a region with a very low seismicity. During

the above mentioned period, the permanently installed Swiss Digital Seismic Network (SDSNet) registered 10 seismic events with local magnitudes M of between 0.9 and 1.9. With the SDSNet located at the surface, the epicenters could be associated with the area of the Faido MFS within an accuracy of one kilometre. As shown above, the cause was clearly associated with the ongoing construction works and the thus triggered stress redistribution process. In parallel, systematic rock burst events started occurring upon exiting the fault zone, clearly implying that a combination of strain burst events (smaller events) and a strike-slip burst mechanism (larger events) – as proposed by [Ortlepp and Stacey \(1994\)](#) and [Kaiser and Cai \(2013\)](#) – is present. In order to gain a clear picture on the involved mechanisms and make predictions on the long-term behaviour of the tunnel (operation stage), the freshly founded Micro-Tremors working group decided to install additional seismic stations at the surface and in the Faido MFS. For precise monitoring and location of the seismic activity sources, a special local seismic network consisting of nine stations at the surface, including one station from the SDSNet, were installed in a circular arrangement 10 to 15 km around the Faido MFS. In addition, two stations were installed at different locations in the tunnels of the Faido MFS. The circular position of the seismic measuring equipment allowed for a precise determination of the epicenters whereas the measuring stations directly above and inside the Faido MFS serve the evaluation of the depths of the micro-tremors' sources. Accurate seismic wave velocities required for the determination of the hypocenter were derived from two calibration shots carried out in the Faido MFS. An average P-wave velocity of 5.33 km/s was calculated. The readings of the measuring stations were integrated in the SED's data acquisition system. The real time transmission of the measuring data guaranteed a continuous survey of the seismic activity allowing for an immediate alert of the responsible organisations such as ATG, supervision and authorities in case of a strong tremor. This was of particular importance for the M2.4 tremor occurring in March 2006.

3.2. Chronology of the seismic events

Fig. 6 shows the development of the number and magnitudes of the recorded micro-tremors as functions of time. The highest seismic activity took place during December 2005, March 2006 and May 2006. The highest magnitude of 2.4 occurred on 25. March 2006 and was perceived at the surface. From October 2005 to February 2008, 112 micro-tremors were recorded.

The magnitudes of most of the tremors were below 1.0. With termination of the excavation in the Faido MFS, the number and magnitudes of the micro-tremors decreased continuously. Since September

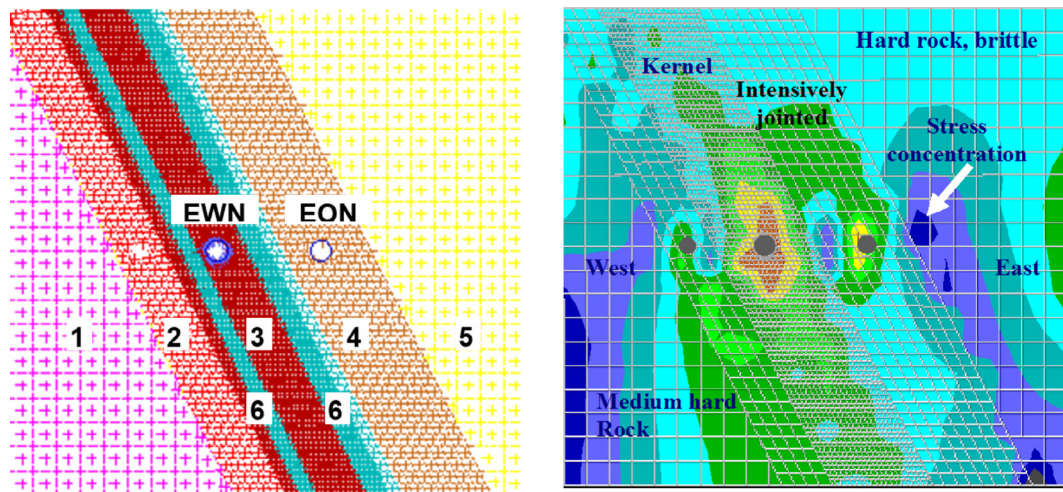


Fig. 5. Left: UDEC Model with the geological regions and the position of the tunnels. Right: Static load case: distribution of the vertical stresses.

2007, no more micro-tremors have been recorded above the measuring threshold of $M = -1.0$ in the area of the Faido MFS.

3.3. Hypocenters

The hypocenter of all micro-tremors registered during October 2005 to February 2008 are depicted in Fig. 7. The micro-tremors are concentrated in the rock mass to the north of the Faido MFS close to the eastern part of the tunnel system with only singular and smaller events south of the Faido MFS and the fault crossing it.

The accuracy of the hypocenters' localisation is less than 100 m and less than 250 m in focal depth as determined by relocation of the calibration shots. Within the error ellipsoid, the tremor sources are at tunnel level.

3.4. Findings from the seismic measurements

The micro-tremors in the northern part of the MFS tend to form clusters i.e. the sources of several tremors are located within the same area. Considering the predominant steep west-east dipping joint system striking sub-parallel to the tunnel axis, shear failures along joints are most likely. The locations of micro-tremor sources in the hard Leventina gneiss to the east of the fault corresponds to the location of the vertical stress concentrations resulting from the computations of the static load case in Fig. 5. There is a general tendency of the micro-tremors to move together with the excavation of the tunnels from the cross-cavern area to the north. Very few micro-tremors occurred in the southern part of the Faido MFS.

The systematic waveform analysis revealed that several families of micro-tremors exist, thereby implying not only the clustering of the locations, but also similar failure mechanisms being triggered over and over again. Thirteen distinct micro-tremor families have been identified

Table 1
Rock and fault zone parameters.

Zone	Rock mass	Young Modulus E [GPa]	Poiss. ratio ν [-]	Friction angle ϕ [°]	Cohesion c [MPa]	Joint friction angle ϕ_j [°]	Joint Cohesion c_j [MPa]
1	Lucomagno gneiss	25	0.20	27	6.4	27	3.2
2	Lucomagno gneiss, jointed	20	0.21	27	4.6	27	2.3
3	Leventina gneiss, intensely jointed (Kernel)	24	0.20	36	3.6	28	1.8
4	Leventina gneiss, jointed	27	0.19	36	8.9	36	4.5
5	Leventina gneiss	35	0.18	36	12.5	36	6.3
6	Leventina gneiss, intensely jointed with kakirite (kernel)	3	0.21	22.5	0.5	20	0.3

(Fig. 8).

3.5. Impact on the construction

During the excavation of the north-eastern section of the MFS, a large number of rock bursts occurred. At that time, 75% of all events took place at the face during the first three hours after a drill-and-blast round and were perceived in the form of vibrations and loud cracking or bangs up to material ejection from the face. In May 2004, a rock burst occurred for the first time in the side wall of the single-track tunnel east/north (EON) that had already been secured for several months. Rock suddenly loosened and the vault deformed over a distance of about 30 m. Some days later, a major rock burst occurred in the single-track tube east/south (EOS), resulting in rock loosening in the left side wall. This also destroyed the shotcrete lining over a length of 30 m.

The damage potential of rock bursts is illustrated in Fig. 9. The left picture shows the damage of the support with a shotcrete plate ejected into the EON. This rock burst occurred together with the M1.9 micro-tremor of July 2005. The EON's invert heave presented in the right picture was caused by the M2.4 earthquake of March 2006. The invert heave caused solely by the seismic impact was smaller than it is shown in the picture, which was taken two days later and captures the subsequent smaller events and associated bulking (Kaiser and Cai, 2013) of the invert material.

3.6. Numerical modelling of the seismicity

The UDEC model similar to the one presented in Fig. 5 has been taken as a starting point for a full dynamic analysis of the events. The excitation wave used at the domain boundary in the model has been delivered from the Swiss Earthquake Service (SED), with particle

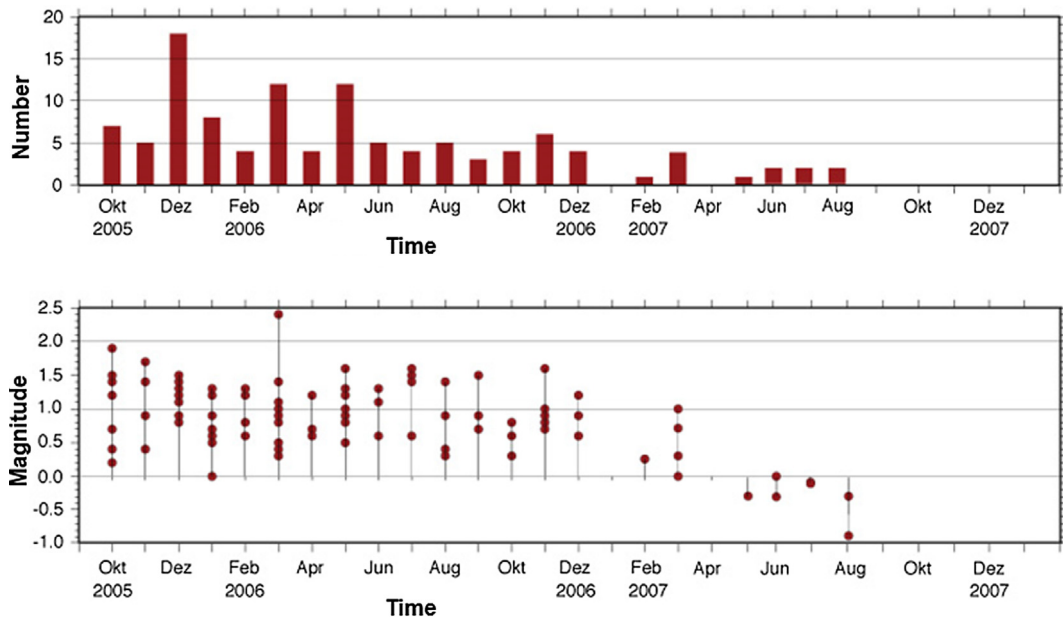


Fig. 6. Chronological development of the number and magnitudes of the micro-tremors.

velocities calculated from the measurements of the M2.4 seismic event (Fig. 10).

The numerical analysis provided impressive results, with a clear anomaly being generated at 0.1359 s after excitation start and giving a direct insight why the failure was triggered in the invert of the tunnel (Fig. 11). Table 2 shows the response of the displacements in the inner lining to the “stress drop” triggered by the seismic event. The highest deformations of 5 mm take place in the east side wall and the invert of the EON tube. The lowest displacements occur in the inner lining of the EWN tube. The internal forces show the same trend as the displacements.

3.7. Discussion of the mechanism involved

As already stressed by many authors, (Huwe and Baltz (2007), Kaiser and Cai (2013), Ortlepp and Stacey (1994), Zhang and Feng (2012)) the rock burst occurrence in complex tectonical regime is governed by many influencing factors, all interacting with each other. Based on the findings presented above, and based on static numerical analysis of the wide area stress field, rigorous seismic monitoring and dynamic analysis with a measured excitation wave, following summary of the mechanisms involved and their interdependencies can be

presented:

- Excavation method: while the blasting causes the formation of micro cracks and strain energy dissipation at the excavation boundary, it also represents man-made micro-seismicity, sometimes triggering additional events. On the other hand, TBM advances are prone to less frequent, but more violent strain bursts, due to the lack of the aforementioned dissipation and higher rates of advance (Zhang et al. (2012a)).
- The presence of a major tectonical fault has two adverse effects on the stress situation in the vicinity of the tunnel: the primary stress state is disturbed in its vicinity and stress concentrations and stress-relieved regions are formed, due to the genesis of discrete structures in its vicinity (for instance: Riedel shear bands). On the other hand, the stress re-distribution process due to the excavation is acutely influenced as well, since the low shear strength of the fault prevents normal stress redistribution. This leads to stress increase in the “pillar” between the fault (or other, associated discontinuities) and the excavation in case of obliquely striking faults AND to a rapid rate of stress increase when closing or leaving a perpendicular fault (due to lack of longitudinal stress distribution).

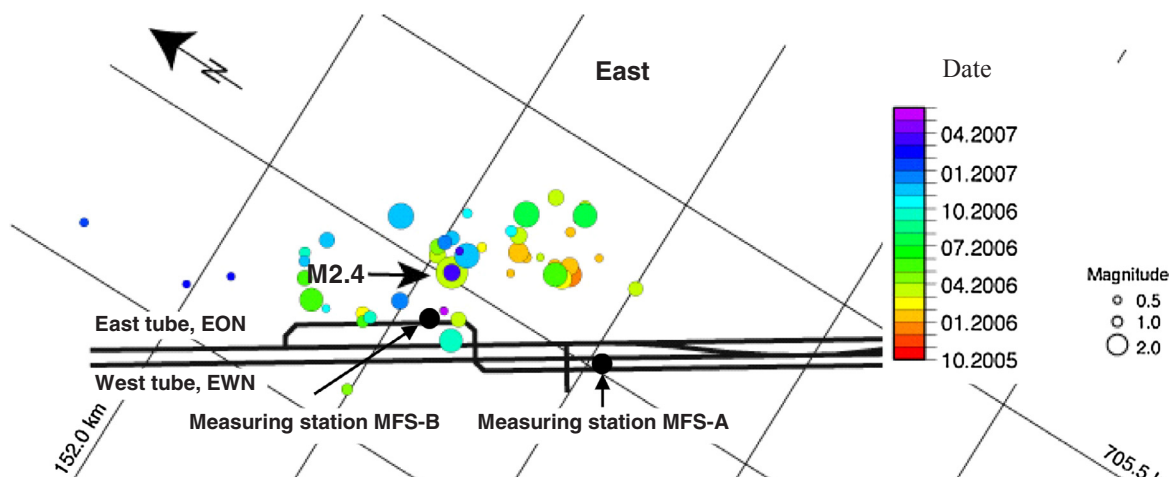


Fig. 7. Epicenters of the micro-tremors from October 2005 to February 2008.

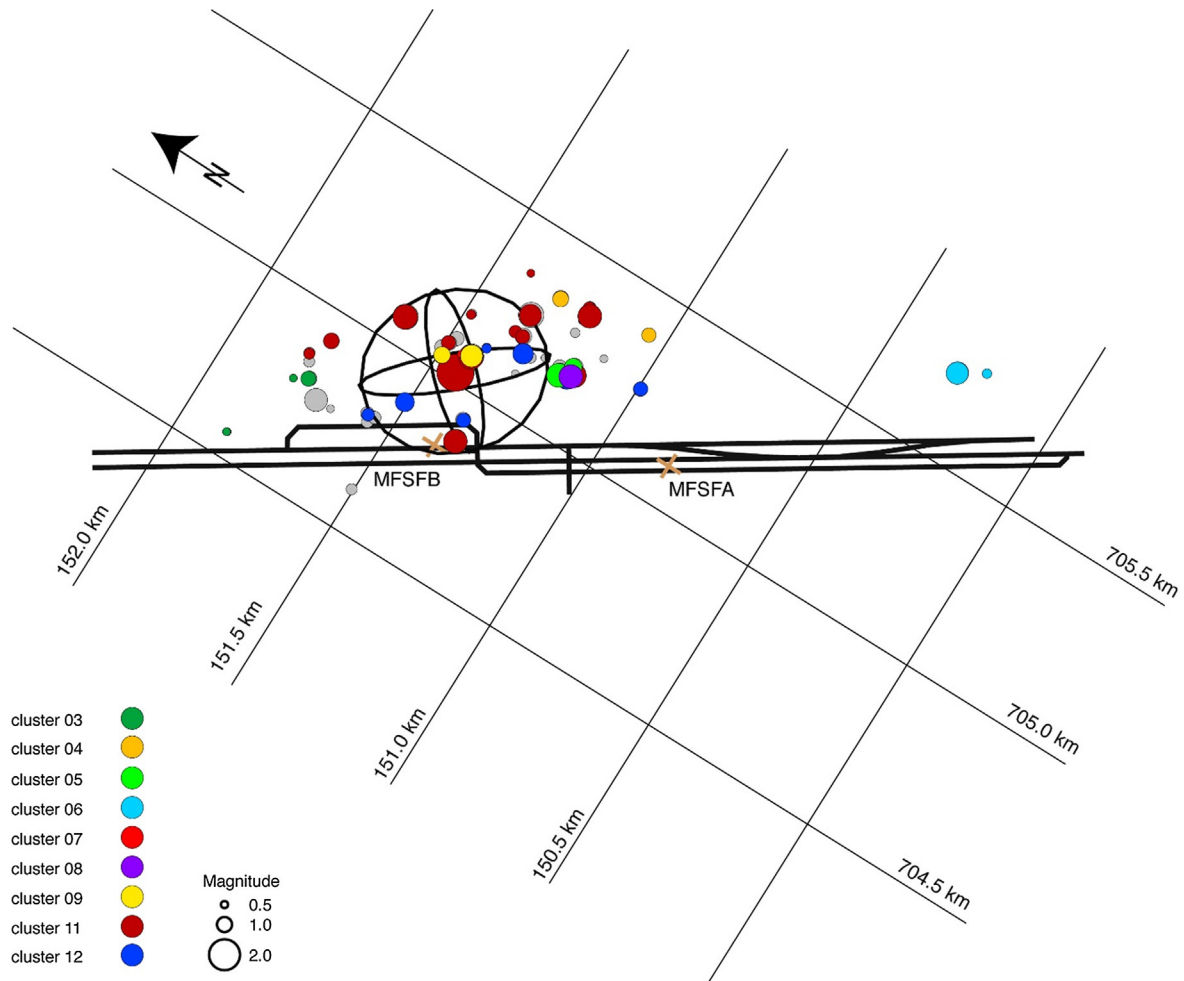


Fig. 8. Hypocenters of the microevents with assigned event family (events without family assignment are depicted grey).

– As shown here, the presence of a major tectonical fault can have a regional, large scale adverse effect as well, in case the fault has been at its “limit state” prior to excavation. As impressively demonstrated by comparing the results of numerical analysis with the hypocenter location (Figs. 5 and 7), the seismic events are aligned with the stress concentration caused by the excavation. This stress change was apparently sufficient to trigger systematic micro-seismic activity until the new stable state was reached. The energy release of these events, in turn, caused the limit state of the rock mass around the excavation to “topple”, leading to the major rock bursts shown above.

A summary of the considerations above and the perceived interactions are shown below (see Fig. 12).

4. Mitigation measures

While designing the appropriate support, one has to be aware of the fact that the rock bursts can neither be exactly predicted nor prevented by excavation support measures. Nevertheless, action must be taken to ensure the safety of workforce and equipment. Constructional adaptations of the support and excluding critical tunnel sections for access were required. A forecast of the rock burst risks was undertaken along



Fig. 9. Single-track tube east/north. Left: damage of the shotcrete support after the M1.9 event. Right: invert failure and bulking after the M2.4 event.

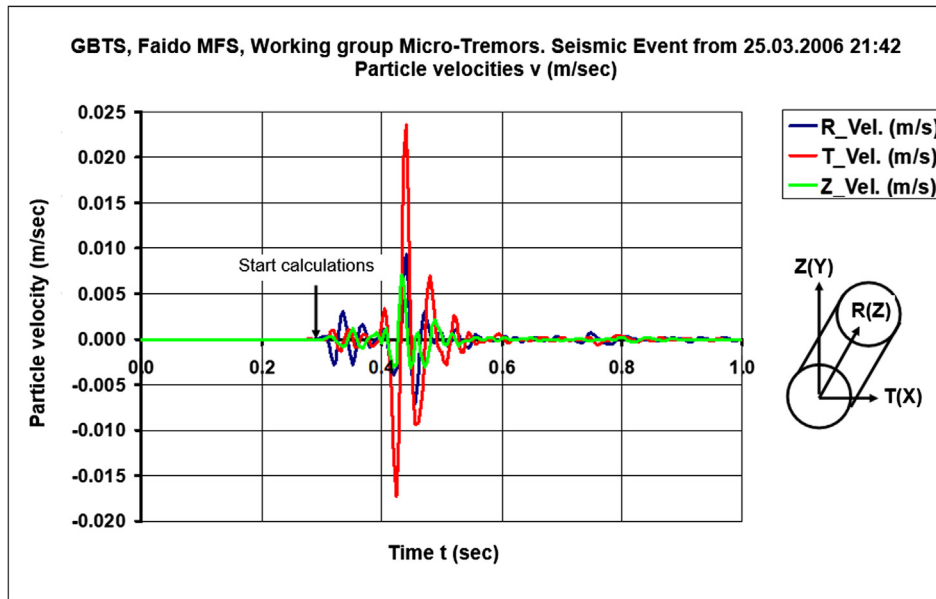


Fig. 10. Results (particle velocities) of the calculation for determining the excitation wave used in the numerical model.

with the envisioned measures. The implemented mitigation measures have been designed in the line with the recommendations of Bräuner (1992), Huwe and Baltz (2007) and Kaiser and Cai (2013). The support has to fulfil the requirements of reinforcing the rock mass, holding it and retaining it in case of major event (Fig. 13).

A rock burst information sheet and a progressive list of measures (Table 3) has been prepared. Specific hazards and the necessary actions were being determined in advance and are continually adapted as new knowledge has been obtained during tunnelling operations. Various preventive measures were prescribed:

- sealing of the face with steel-fibre shotcrete (to prevent loosening of small particles from the face)
- face anchors with large anchor plates
- leaving a pile of material in front of the face (to prevent access close to the face)
- switching to top heading excavation method
- arched face formation (to anticipate the excavation form usually resulting from stresses)
- prohibiting of manual work around the face for the first three hours after a drill-and-blast round

Table 2

Maximal displacements dx, dy in the inner lining as a result of the simulated M2.4 seismic event.

Max. Displacements		Max. dx mm		Max. dy mm	
Tunnel	Segment	–	+	–	+
EON	Side wall east	5.0	1.8	1.3	1.7
	Top heading	2.8	3.0	1.3	1.7
	Side wall west	3.8	3.5	1.0	2.0
	Invert	5.0	1.0	0.7	1.9
EWN	Side wall east	2.5	1.8	1.6	0.4
	Top heading	2.2	1.2	1.8	0.9
	Side wall west	2.1	1.4	0.8	0.7
	Invert	2.3	0.2	1.6	0.5

In addition, excavation support measures were altered to meet the different levels of rock burst risk. Special yielding support elements were used to absorb dynamic loading, such as rock bolts (Swellex or Yielding Swellex bolts) and flexible steel arches.

During the excavation, the potential of heavy rock bursts in the different parts of the MFS were predicted, the necessary support

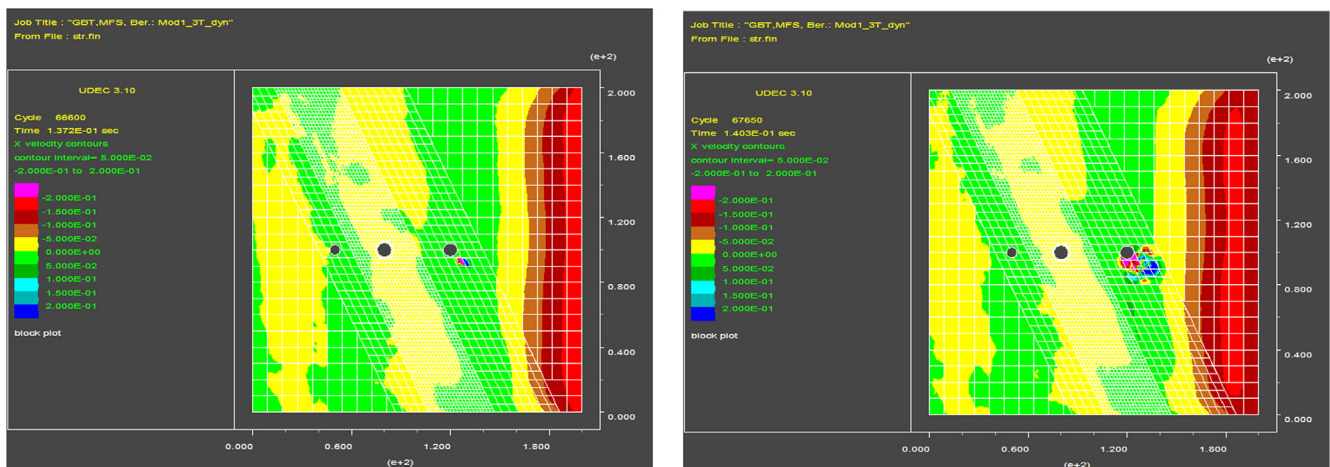


Fig. 11. Contour plot of horizontal velocities (v_{xx}) in the model. Left. Start of anomaly generation at $T = 0.1359$ s. Right: anomaly propagation at 0.1403 sec.

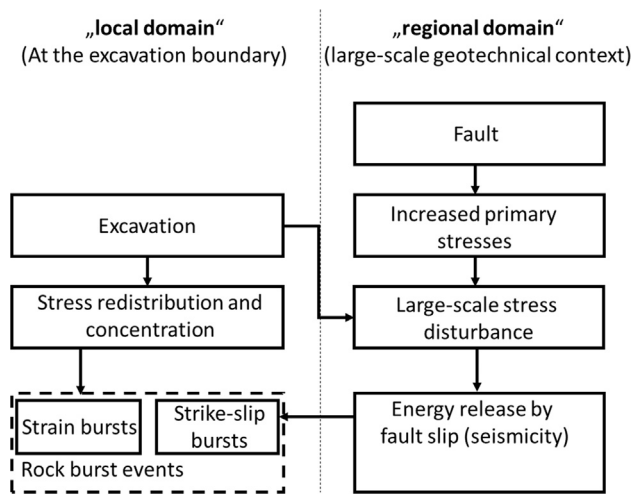


Fig. 12. Chart of qualitative interactions between the in-situ conditions and the excavation.

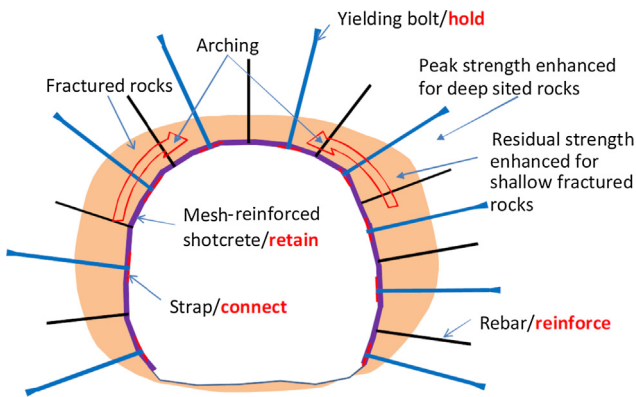


Fig. 13. Schematic of a reliable support system in burst-prone rock mass, after Kaiser and Cai (2013).

measures and additional means were fixed. This led to the closure of some sections for all traffic with major impact on the logistics of the site. During the construction works at the Faido MFS, several hundred rock bursts occurred. With the aforementioned countermeasures, no injuries or accidents due to rock burst were reported.

5. Conclusions

Rock bursts cannot be avoided. During construction, precaution measures such as closing of critical sections and flexible support consisting of flexible rock bolts and steel arches are to be applied. The potential for occurrence of strain bursts can be reliably identified, along the lines of criteria presented by Wang and Park (2001) and Singh (1989). Both publications allow a sound classification of rock burst potential based on the properties of the intact rock. However, more complex situations, as the strike-slip mechanism presented above, can't be predicted due to a vast amount of uncertainties. However, the design methodology and the experience with regard to risk mitigation of rock burst is sufficient to allow for safe and economical tunnelling.

If considering only the discussed project, following additional conclusions lie at hand:

- The dynamic impact on the lining of a tunnel in front of a weak zone and exposed to a more or less unhindered micro-tremor wave is considerably higher compared to the impact on a tunnel lining in the 'shelter' of a weak zone.
- A seismic wave is deviated by a weak zone. With the orientation of the weak zones present in the Faido MFS, additional anomalies in the tunnel vicinity are likely, causing larger rock bursts.
- The specification of the design micro-tremor for the Faido MFS is conservative (the largest event has been taken into account as a design basis). Excluding the additional loading due to a spontaneous 'stress drop' in the direct vicinity of a tunnel, there was and is no need for improving (thickness, additional reinforcing) the linings designed for the static load case in the Faido MFS.
- The risk of a major fault slip and subsequent damage to the inner lining is regarded as residual risk and has been accepted by the client.

Table 3
Rock burst classes, perceived phenomena and measures.

Term (event)	Perceived phenomena	Measures
E1 Release	<ul style="list-style-type: none"> - Cracking sound - Rumbling 	<ul style="list-style-type: none"> - Document observations in shift and daily report of contractor - Intensify observations - Partial excavation (top heading) - Overhead protective mesh over entire crown - Shotcrete on face, vaulted face - Face anchor bolts
BS1 Light rock burst	<ul style="list-style-type: none"> - Vibrations - Dust dispersion - Heavy face spalling during loosening in the form of plates of up to about 5 m³ and about 1 m deep 	<p><u>In addition to E1:</u></p> <ul style="list-style-type: none"> - Strengthen face bolting - Leave wedge of material in front of face - Intensify and strengthen system bolts - Strengthen overhead mesh
BS2 Medium rock burst	<ul style="list-style-type: none"> - Extreme vibrations - Vibrations 3–6 h after – excavation - Dust clouds from crown - Face spalling of less than 5 m³ prior to loosening - End anchor plates 	<p><u>In addition to BS1:</u></p> <ul style="list-style-type: none"> - Denser, yielding rock burst anchoring
BS3 Extreme rock burst	<ul style="list-style-type: none"> - Extreme vibrations - Several successive vibrations - Concussions after more than 3 h - Shotcrete spalling - Cracking of shotcrete on face - Face spalling greater than 5 m³ before loosening - Overbreak formation - Anchor heads torn off near abutment 	<p><u>In addition to BS2:</u></p> <ul style="list-style-type: none"> - Denser bolt pattern if damage pattern - Re-pattern bolting/strengthening - Face bolting, reduction - Bolt spacing, reduction - Pressure-relief blasting - Submit event report (short report)

References

- Bräuner, G., 1992. Gebirgsschläge und ihre Verhütung. Taschenbuch. Verlag Glückauf Essen. ISBN 978-3773905864.
- Huwe, H.-W., Baltz, R., 2007. Sicherheit erfordert Sachverstand: Sachverständigenbericht 2005-2006 der Fachstelle für Gebirgsschlagverhütung. Glückauf Essen 143, 334–336 Deutsche Bergbautechnik GmbH.
- Ingenieurgesellschaft Gotthard – Basistunnel Süd IGGTS, ATG, Basler&Hofmann, 2008. GBT, TA Faido, Multifunktionsstelle (MFS) – Schlussbericht der Arbeitsgruppe Mikrobeben (not published final report of the working group “micro tremors”).
- Kaiser, P.K., Cai, M., 2013. Keynote lecture on rockburst damage mechanisms and support design principles. Proceedings of RaSiM 2008.
- Ortlepp, W.D., Stacey, T.R., 1994. Rockburst mechanisms in tunnels and shafts. Tunnell. Underg. Space Technol. 9, 59–65 Elsevier Science.
- Singh, S.P., 1989. Classification of mine workings according to their rockburst proneness. Mining Sci. Technol. 8, 253–262 Elsevier.
- Wang, J.-A., Park, H.D., 2001. Comprehensive prediction of rockburst based on analysis of strain energy in rocks. Tunnell. Underg. Space Technol. 16, 49–57 Elsevier.
- Zhang, C., Feng, X., Zhou, H., 2012a. A top pilot preconditioning method for the prevention of extremely intense rockburst in deep tunnels excavated by TBMs. Rock Mech. Rock Eng. 45, 289–309 Springer Verlag.
- Zhang, C., Feng, X., 2012. Case histories of four extremely intense rockbursts in deep tunnels. Rock Mech. Rock Eng. 45, 275–288 Springer Verlag.